Available online at www.sciencedirect.com

Catalysis Today 89 (2004) 117–126

CATALYSIS TODAY

www.elsevier.com/locate/cattod

Plasma–catalyst interactions in the treatment of volatile organic compounds and NO_x with pulsed corona discharge and reticulated vitreous carbon Pt/Rh-coated electrodes

Michael J. Kirkpatrick, Wright C. Finney, Bruce R. Locke*

Department of Chemical Engineering, FAMU-FSU College of Engineering, Florida State University and Florida A&M University,
2525 Pottsdamer Street, Tallahassee, FL 32310-6046, USA

Abstract

The combination of pulsed positive streamer corona discharge with a platinum–rhodium catalyst was investigated for removal of toluene, acetonitrile, and nitrogen oxides. The reactor used consisted of two parallel disks made from reticulated vitreous carbon, with the downstream disk coated with platinum and rhodium. Removal of contaminants was measured with and without plasma over a range of temperatures, and several interesting phenomena were observed which differed between the three species. Results indicate that the catalyst is capable of both reduction of nitrogen oxides and oxidation of hydrocarbons. In addition, the combination of the active catalyst with the plasma discharge was found to either enhance or interrupt catalyst activity depending on which contaminant was considered and the catalyst temperature.

Keywords: Non Thermal Plasma; Pt/Rh; Reticulated vitreous carbon

1. Introduction

Heterogeneous catalysts have been used to treat combustion exhaust gases and the emissions from numerous other air pollution sources for many years [1]. More recently, non-thermal plasma processes have been under intensive investigation for the removal of nitrogen oxides, sulfur dioxide, and many organic compounds (e.g., toluene, trichloroethylene, vinyl chloride) and other inorganic species (e.g., mercury) from industrial and commercial gas phase sources [2]. These processes include pulsed corona discharge [3,4], dielectric barrier discharge (DBD) [5–8] and electron beam processes [9–11]. Although the electrode surfaces in such systems may have very large temperatures, and, in some select applications, products may form and react on the surface of the electrode, typically the key chemical transformations in conventional plasma processes for waste control occur in the bulk gas.

Recent studies of DBD and corona technologies have considered the interaction of non-thermal plasma with catalysts [12–29]. It has been suggested in these studies that the addition of a heterogeneous catalyst in or near to the plasma discharge can have a synergistic effect on contaminant removal, although rigorous investigation of possible mechanisms for such an effect have only recently begun [22,29].

The present study focuses on a platinum–rhodium catalyst supported on reticulated vitreous carbon (RVC), a material that may be used as an electrode material in pulsed corona discharge reactors [15,30,31]. The removal of acetonitrile, nitrogen oxides, and toluene are studied with plasma, catalyst, and combined plasma–catalyst treatments. Nitrogen oxides and toluene were chosen based on the availability of data for comparison in the literature. Acetonitrile was interesting in that it has an ionization energy higher than that of oxygen, a property that has been shown to be important for plasma treatment [32]. An ionization energy higher than that of oxygen means that charge transfer reactions between oxygen and acetonitrile are not allowed, and so any removal would be due to radical reactions. Other compounds with higher ionization energies than oxygen such as sulfur dioxide and methane have been shown in [32] to be more difficult to remove under plasma treatment in oxygen rich gases than other compounds, the majority of which have lower ionization potentials than that of oxygen.

Several studies have demonstrated plasma-enhanced catalysis. Among the studies discussed below, and others,

---

* Corresponding author. Tel.: +1-850-410-6165;
fax: +1-850-410-6150.
E-mail address: locke@eng.fsu.edu (B.R. Locke).

0920-5861/$ – see front matter © 2003 Elsevier B.V. All rights reserved.
doi:10.1016/j.cattod.2003.11.017

there are wide variations in catalyst type, reactants, plasma generation type, temperature, plasma reactor/catalyst geometry, and other factors affecting the plasma–catalyst interaction.

Roland et al. [22] discuss evidence for two types of plasma-enhanced catalysis. Evidence for the first type arises from a set of experiments with *n*-eicosane ($C_{20}H_{42}$), immobilized on the catalyst (α-alumina, γ-alumina, silica gel, and quartz). These experiments provide evidence that the immobilized hydrocarbon is degraded by oxygen radicals and is unaffected by ozone. Another result is that the γ-alumina catalyst degrades ozone, forming oxygen radicals, again leading to the degradation of the adsorbed hydrocarbon. In the second type of plasma-enhanced catalysis, Roland et al. [22] found that pretreatment of a catalyst with plasma can alter the surface concentration of the oxidizing species such as atomic oxygen.

Studies with DBD combined with a proprietary catalyst by Hoard and Balmer [17] showed significant removal of total NO_x from diesel exhaust. Further studies by the same group demonstrated the effect of multiple plasma and catalyst stages and the effect of catalyst temperature and hydrocarbon levels on NO_x conversion toward N_2O and HCN, and by inference N_2. This group points out a target energy efficiency for such a process and is approaching that value in their latest studies [33].

Ogata et al. [25] present evidence of plasma-enhanced surface reactions for the removal of gas phase benzene. Key findings of these experiments are that adsorbed benzene is oxidized only when the catalyst is in close proximity to the plasma and that the plasma somehow changes the adsorption of benzene to the catalyst, perhaps by creating new adsorption sites.

Other studies have found that the presence of a catalyst may affect properties of the plasma [34]. In addition, multiple plasma and catalyst reactors in series [33] and the addition of ammonia to the system [16,35] have been studied. In addition to the variables discussed above, gas composition, catalyst temperature, and plasma energy density are important variables in the investigation of plasma–catalyst interactions.

The present study follows work performed using RVC as an electrode material in pulsed corona discharge [15,31]. Data from that work suggested an interaction between nitrogen oxides and the carbon electrodes that was caused by the plasma discharge. This possible interaction provided a rationale for adding catalytic materials to the pulsed corona reactor RVC electrodes.

2. Experimental

The experimental setup for the present study consists of upstream gas flow control and measurement, a heated pulsed streamer corona reactor, and downstream gas composition analysis. The heated pulsed streamer corona reactor can be operated with and without a catalyst disk used as the down stream grounded electrode. Earlier experimental work on NO_x removal using the same power supply has been reported [31,36].

2.1. Pulsed streamer corona reactor

A schematic of the heated pulsed streamer corona reactor is shown in Fig. 1. The reactor body is constructed of glass. The plasma discharge occurs between two RVC (Ultramet, Pacoima, CA) disks 10 cm in diameter and 1 cm thick. Teflon is used as both a gasket and to prevent the discharge from propagating along the glass walls of the reactor, thereby creating homogeneously distributed streamers in the center of the reactor. The area of the electrodes not blocked by the Teflon gasket is 20 cm^2, and the RVC disks are placed

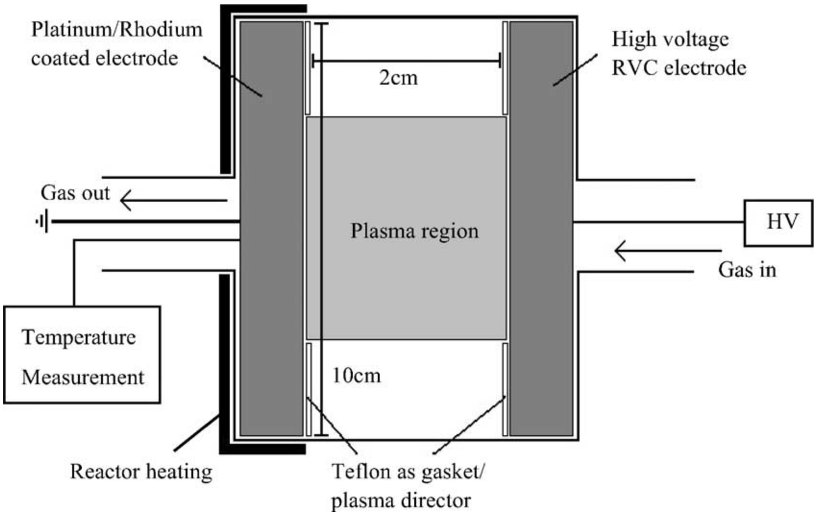

Fig. 1. Schematic representation of the heated plasma–catalyst reactor. The catalyst disk may be replaced by an uncoated carbon disk for control experiments.

2 cm apart, giving a total plasma volume of approximately 40 cm^3.

The reactor is heated using resistive heating tape wrapped on the exterior of the reactor and insulated with a layer of fiberglass ribbon. Temperature measurements are made using a thermocouple that is placed in contact with the downstream side of the catalyst disk. Measurement of temperature was not possible when the plasma was on due to RF noise created by the pulsed power supply.

2.2. Electrode materials

In all experiments, the high voltage electrode was a RVC disk with 10 pores per inch (ppi) obtained from Electrosynthesis Inc. (Lancaster, NY). The structure of the RVC disk is such that there are many sharp edges and points along the plane of the electrode facing the discharge region. Streamers are observed to consistently form at these points during the plasma operation. The grounded electrode used was either a 10 ppi disk similar to the high voltage electrode, or a 100 ppi disk with catalytic coating obtained from Ultramet Inc. (Pacoima, CA).

The catalyst disk was prepared by Ultramet Inc. by using 100 ppi RVC as a substrate and first applying a graphitic layer that increased surface area to approximately 50–70 m^2/g, and thereafter applying platinum and rhodium with a 5:1 ratio onto the graphitic coat, a ratio recommended by Ultramet Inc. for lean NO_x catalysis. The graphitic coat on the RVC is stable to at least 250 °C, while the RVC itself is stable up to 500 °C. The maximum temperature that this catalyst can withstand for extended periods is not known. The amount of metal applied to each disk was estimated by Ultramet Inc. to be approximately 1–2 g. Images of the surface of this material made with a scanning electron microscope are shown in Fig. 2.

The plasma discharges for the two cases of the 10 ppi non-catalytically coated RVC disk and the catalyst coated RVC disk as grounded electrodes were found to be similar as determined by current and voltage waveforms and visual observations.

2.3. Gas composition and analysis

Gas flow is controlled with mass flow controllers (MKS Instruments, Andover, MA). The gases are supplied from either a high purity gas cylinder or, as in the case of toluene and acetonitrile, by bubbling nitrogen through liquid organic in a gas wash bottle. The carrier gas for the VOC experiments (toluene and acetonitrile) was dry synthetic air. For the NO_x experiments, ~130 ppm NO/10% O_2/balance N_2 gas was used. For all experiments presented here, a gas flow rate of 1 l/min was used giving a residence time of 2.4 s in the plasma zone between electrodes and ~1.2 s in the catalyst of the downstream RVC electrode. It should be noted here that the addition of water vapor to the gas would likely have significant effects on the chemistry of both plasma and catalyst, and that water would be present in most applications.

Gas sampling cells are located both up and downstream of the reactor. Samples are taken from these cells using a Hamilton 250 μl syringe and injected into a Perkin Elmer Autosystem XL gas chromatograph equipped with a flame ionization detector and thermal conductivity detector. Compounds measured or detected using the GC in this work included toluene, acetonitrile, ethylene, carbon dioxide, nitrous oxide, and a few unknown byproducts of the degradation of those compounds. Carbon monoxide and carbon dioxide are measured using a MultiRAE CO/CO_2 monitor (RAE Systems Inc., Sunnyvale, CA). This monitor measures CO_2 using IR absorbance and CO using a proprietary non-IR method. Certain compounds such as hydrogen and ethylene interfere with CO measurements made by this device. Nitrogen oxide and nitrogen dioxide are measured using a chemiluminescence NO_x Model 42H monitor (Thermo-Environmental Instruments).

2.4. Pulsed power supply and electrical characteristics

The electrical system used is similar to the one used in our previous work [15,31,36]. The electrical discharge produced by this circuit in the RVC reactor had rise time on the order of 20 ns, pulse width of 500 ns, and energy of

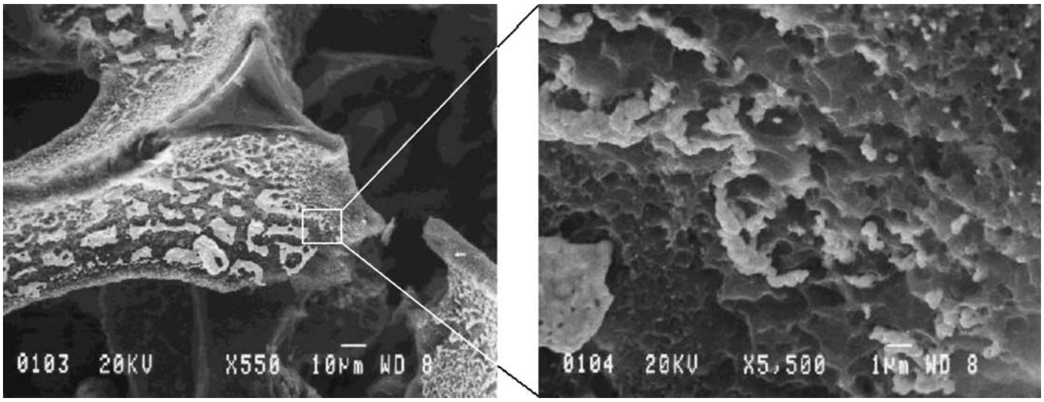

Fig. 2. SEM of catalyst disk surface. Islands of metal can be seen on the carbon support.

~40 mJ/pulse. The experiments are conducted at a constant frequency of 60 Hz and an applied voltage of ~33–36 kV. The resulting energy density applied to the gas in this work is ~140–150 J/l.

2.5. Methods for measurement of catalyst activity and plasma–catalyst interaction

The catalyst disks are characterized for their activity in the absence of plasma toward removal of the contaminant compounds through temperature ramp experiments. In these experiments, the temperature of the reactor is increased and the outlet concentration of the contaminant is monitored over a range of temperatures.

After determination of the temperature window under which the catalyst is active in the removal of the compound of interest, combined plasma–catalyst experiments are performed in that temperature range. For plasma–catalyst experiments, the reactor is held at constant temperature. Once the outlet concentration of the contaminant and observed byproducts are steady, the pulsed streamer corona discharge is turned on and the concentrations of reactants and products are monitored for a specific time interval, typically 20 or 40 min. After the plasma is switched off, the outlet concentrations and reactor temperature are monitored until they stabilize to their initial values.

3. Results and discussion

3.1. Acetonitrile removal

Acetonitrile (CH_3CN) is a volatile organic compound with vapor pressure of 0.11 bar at standard conditions. The ionization potential of acetonitrile is 12.20 eV, compared with 12.06 for the oxygen molecule. Fig. 3 shows acetonitrile removal as a function of temperature with the platinum–rhodium catalyst. Acetonitrile removal begins at about 160 °C, and the amount of removal increases until almost total removal occurs at 250 °C. A summary of data for both catalyst and plasma–catalyst removal of acetonitrile is shown in Fig. 4. The removal of acetonitrile by plasma alone is roughly the same at room temperature and at 210 °C. At this temperature, the catalyst alone removes roughly 70% of the inlet acetonitrile. When plasma is turned on in the region adjacent to the catalyst disk, another ~50 ppm of acetonitrile is removed. This is the same amount removed by the plasma when the catalyst is not present. Thus, acetonitrile removal for this case appears to be the linear combination of the removals observed for plasma and catalyst treatment alone. Carbon dioxide and nitrous oxide byproducts were measured for acetonitrile removal. Again, the production of byproducts is the linear combination of the combination of the two processes. For this reactor geometry, the contact area between plasma and catalyst is at maximum 20 cm^2. It was considered that synergy might be observed at higher flow rates because of higher transport from the plasma to the interior of the catalyst, but an experiment at 10 l/min showed the same linear combination discussed above.

It is not clear if the ionization potential of acetonitrile has an effect on its behavior under combined plasma–catalyst treatment. However, it should be noted that the plasma treatment is not as effective for acetonitrile as for toluene under similar conditions, an observation which agrees with the hypothesis of Krasnoperov discussed in Section 1 [32]. The *G*-value (one unit for energy efficiency of contaminant removal) calculated for acetonitrile removal at room

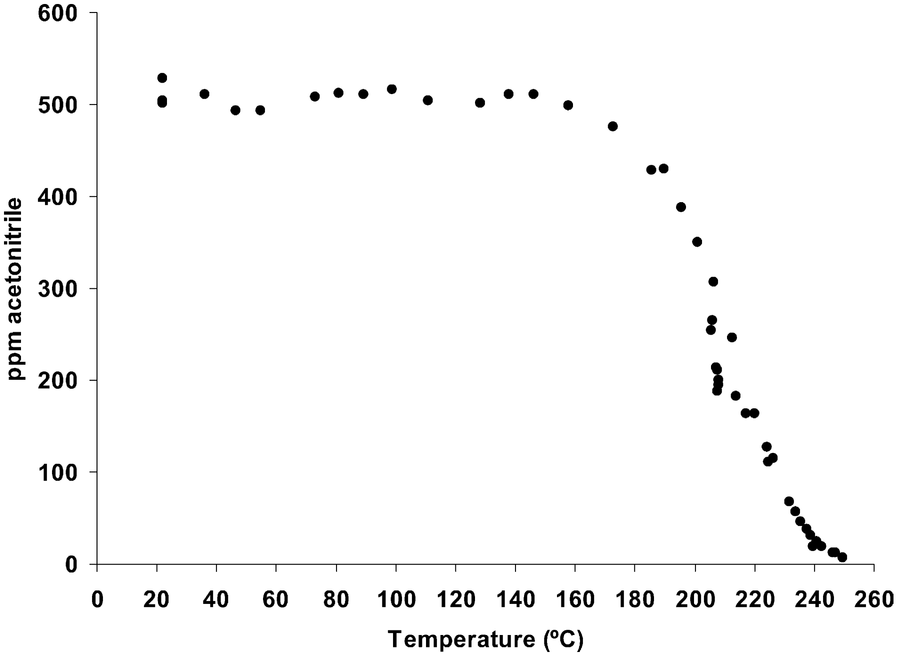

Fig. 3. Light off curve for acetonitrile in dry synthetic air with Pt/Rh disk at total gas flow rate of 1 l/min.

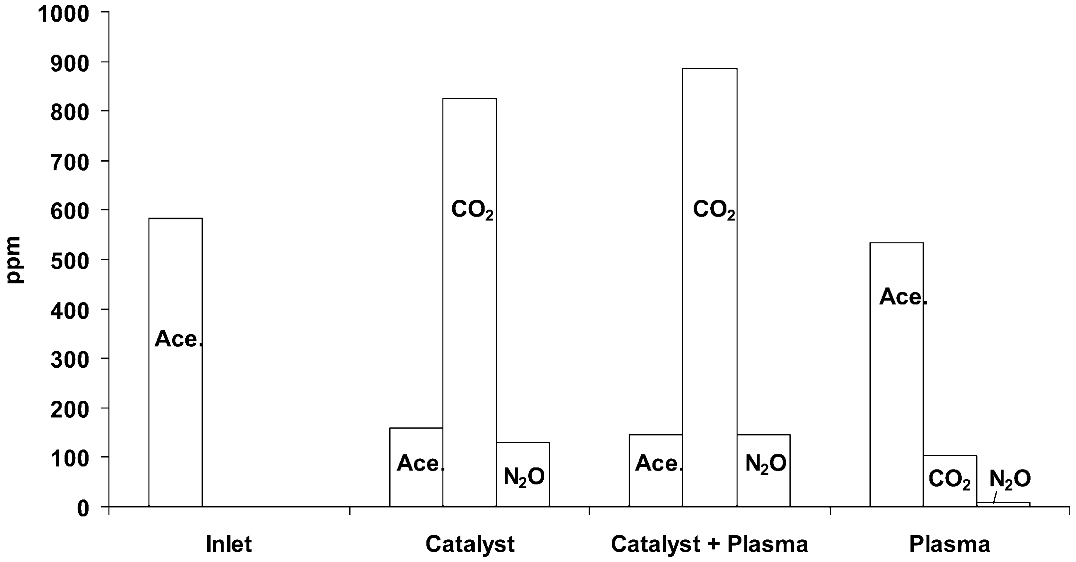

Fig. 4. Histogram of acetonitrile data for plasma, catalyst, and combined plasma–catalyst treatment at 210 °C.

temperature is ~0.09 mol/100 eV, a value which falls near to the 0.1 mol/100 eV delineation proposed by Krasnoperov between the two categories of compounds defined by their ionization potentials relative to the oxygen molecule.

3.2. NO$_x$ removal

A summary of data for nitrogen oxide removal is shown in Fig. 5. A reducing agent such as ethylene is necessary for the catalyst to be active toward reduction of nitrogen oxides as shown in the reaction scheme (R1)–(R5) taken from the review by Kaspar et al. [37]. Asterisks represent surface-bound species. The reaction set (R1)–(R5) demonstrates the necessity of a reductant, such as HC, to free surface sites, O* to S, for NO adsorption. In the present experiments with the Pt/Rh catalyst in the absence of ethylene there was little or no NO conversion. As Kaspar points out, NO conversion typically reaches a maximum at the temperature at which 100% hydrocarbon conversion is observed. Above this temperature, NO is oxidized to NO$_2$ by excess oxygen:

$$\mathrm{HC} + \mathrm{O}^* \rightarrow \mathrm{CO_2} + \mathrm{H_2O} + \mathrm{S} \tag{R1}$$

$$\mathrm{NO} + \mathrm{S} \rightarrow \mathrm{NO}^* \tag{R2}$$

$$\mathrm{NO}^* \rightarrow \mathrm{N}^* + \mathrm{O}^* \tag{R3}$$

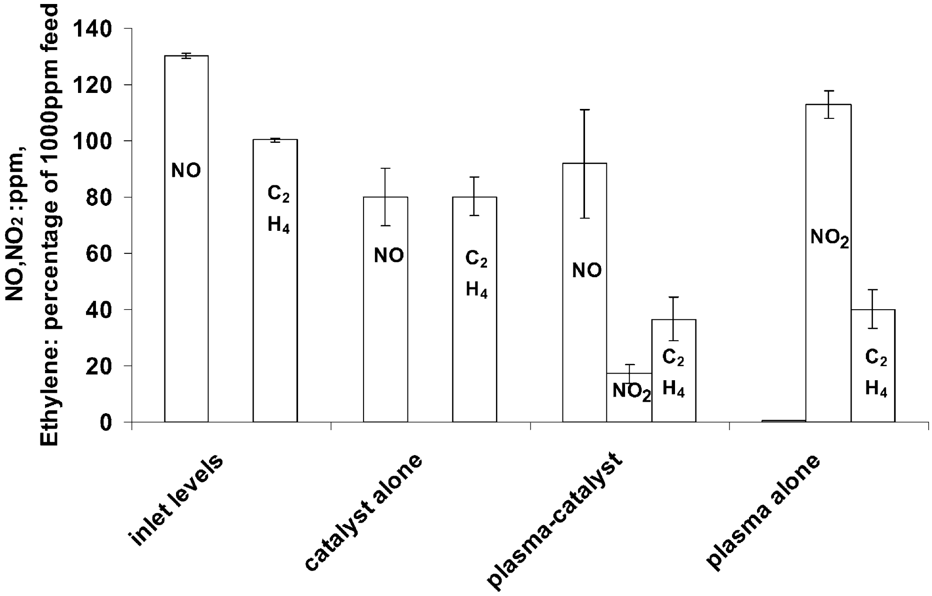

Fig. 5. Histogram of NO/ethylene removal for catalyst, plasma, and combined plasma catalyst treatment at 140 °C.

$$N^* + N^* \rightarrow N_2 + 2S \tag{R4}$$

$$NO^* + N^* \rightarrow N_2O + 2S \tag{R5}$$

The concentrations of NO, NO_2, and ethylene for the catalyst alone, plasma–catalyst combination, and plasma alone cases are shown along with the feed concentrations in Fig. 5. The catalyst alone removes about 40% of the NO and 20% of ethylene at 140 °C without producing any NO_2. Subsequent experiments have shown that up to 40% of the removed NO is converted to N_2O. Molecular nitrogen was not measured. When the plasma is turned on with catalyst at 140 °C, ethylene removal doubles, but the concentration of NO rises slightly, and about 15 ppm NO_2 is emitted. In the plasma alone case, NO is converted completely into NO_2, and ethylene is removed at a rate similar to the combined plasma–catalyst case. The fate of the removed ethylene was measured in follow-up experiments and it was found that for both the catalyst and the plasma–catalyst experiments, conversion to CO_2 was between 95 and 100%. In the plasma alone case, however, the selectivity toward CO_2 was much lower—as little as 10%. It is likely that in this case the fate of the majority of the removed ethylene is to partially oxidized hydrocarbons or carbon monoxide, but these have as yet to be identified or measured.

The interactions between the plasma and this catalyst for NO_x removal can be partially explained as follows. Upstream of the catalyst ethylene is removed or partially oxidized by the plasma. The resulting lower level of ethylene exposed to the catalyst leads to lower NO conversion by reducing the number of surface sites available for NO adsorption, i.e. lowering the rate of reaction (R1). The above argument does not explain the lower level of NO_2 in the plasma–catalyst case compared to the plasma alone case. Plasma alone has the effect of converting NO to NO_2, while in the plasma–catalyst case, significantly less NO_2 is seen at the outlet than in the plasma alone case. The catalyst therefore is converting the NO_2 produced in the plasma back to NO. It is presently unclear whether this reaction is promoted by the plasma through reduction with the partially oxidized hydrocarbon, or if the catalyst is active toward the $NO_2 \rightarrow NO$ reaction in the absence of plasma.

Other evidence suggests that NO_2 may play a role in the surface reactions for the catalytic removal of NO/ethylene. When the supply of ethylene to the catalyst is set to zero under conditions similar to those shown in Fig. 5 for the catalyst alone case, NO_2 is desorbed from the catalyst and NO removal returns to zero much more slowly than the time required for ethylene levels in the reactor to reach zero as shown in Fig. 6. This suggests that NO is oxidized first to NO_2 upon being adsorbed onto the metal (R6), or that adsorption occurs via an adsorbed oxygen atom leading to surface-bound NO_2 (R7). When ethylene is present in the gas, no NO_2 is detected at the reactor outlet, suggesting that the surface phase NO_2 is reduced by the hydrocarbon as in (R8):

$$NO^* + O^* \rightarrow NO_2{}^* \tag{R6}$$

$$NO + O^* \rightarrow NO_2{}^* \tag{R7}$$

$$NO_2{}^* + HC \rightarrow N^* + CO_2 + H_2O \tag{R8}$$

Further characterization of this catalyst is necessary to fully understand the interaction of plasma and catalyst for NO_x removal. Experiments using NO_2 as the feed gas can elicit some information about the activity of the catalyst for conversion of NO_2 to NO, which is indirectly implied by the data using NO as the feed gas.

The experiments on nitrogen oxides leave many questions on the mode of plasma–catalyst interaction in this system. The results imply that the catalyst reduces NO_2 to NO when combined with the plasma. Further work using NO_2 as an

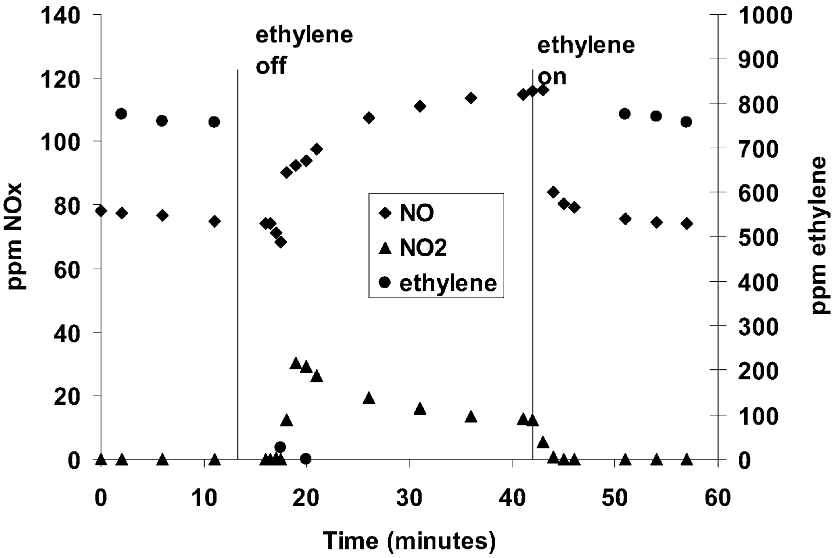

Fig. 6. Time-course data for catalyst only treatment of NO/ethylene at 140 °C showing NO_2 desorption upon removal of ethylene from the feed gas.

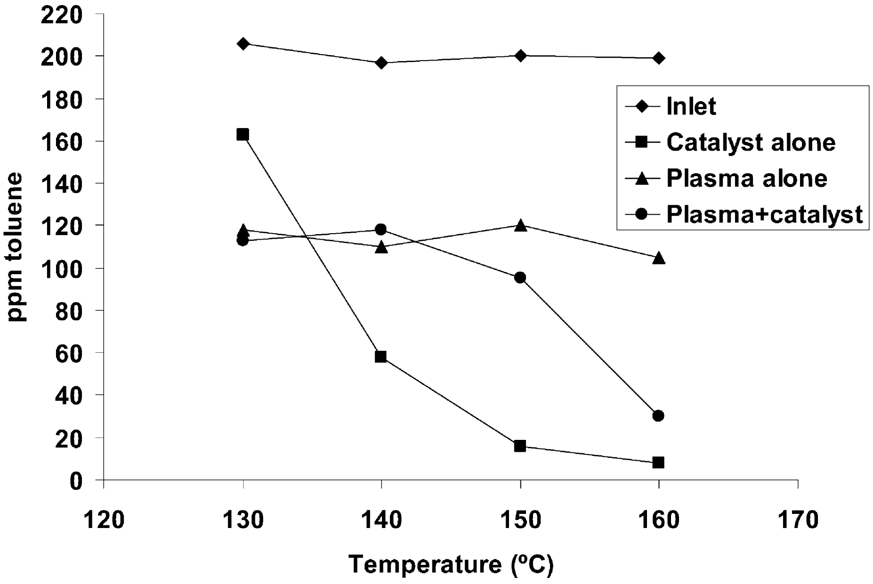

Fig. 7. Toluene concentration vs. temperature for catalyst, plasma, and combined plasma–catalyst treatment.

inlet gas and reversing the orientations of the electrodes relative to the gas flow in the reactor (so that the catalyst is upstream of the plasma) will be done to elicit more information on this system.

3.3. Toluene removal

Data on toluene removal by the catalyst alone, plasma alone, and combined plasma–catalyst treatment as functions of catalyst temperature are shown in Fig. 7. Over the temperature range of 130–160 °C, plasma treatment removed 40–50% of the inlet toluene. At 130 °C, the catalyst removes about 25% of toluene. When plasma is applied in combination with the catalyst at this temperature, the toluene removal increases roughly to that observed for plasma alone. In contrast to the apparent linear combination of removal of acetonitrile for plasma and catalyst, the toluene removal at 130 °C is less than the linear combination of the two individual processes. At 140 °C, removal of toluene by the catalyst increases to about 70%, the combined plasma–catalyst treatment results in roughly the same removal as observed at 130 °C. At 150 and 160 °C, the plasma–catalyst treatment approaches that of the catalyst alone and exceeds the removal due to plasma treatment alone. The removal for

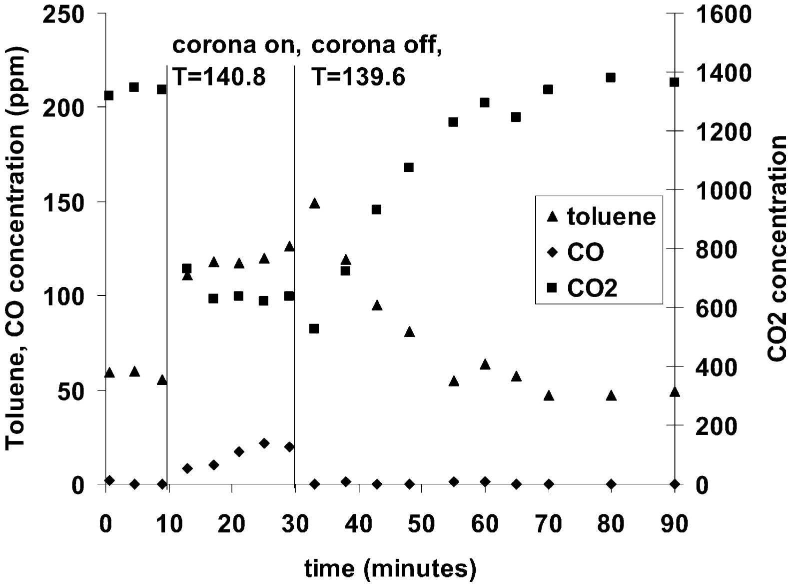

Fig. 8. Time-course data for toluene removal showing time needed for catalyst to return to original activity after plasma is turned off.

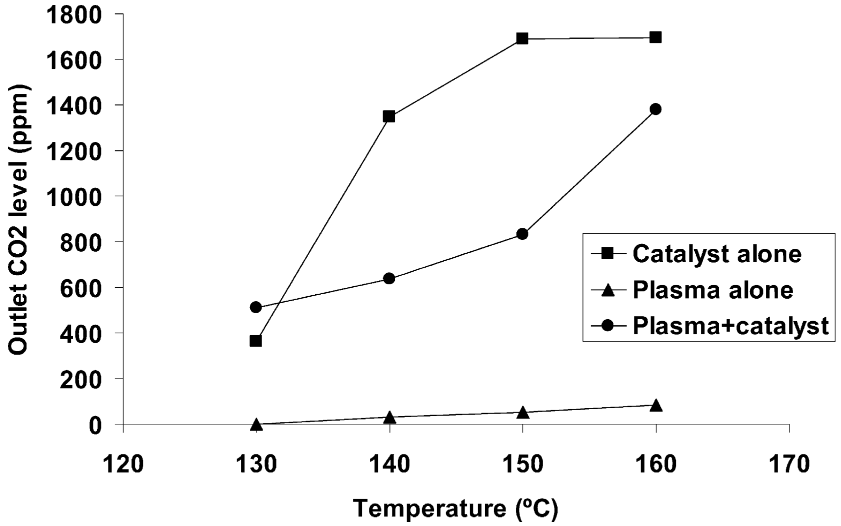

Fig. 9. CO_2 concentration at reactor outlet for catalyst, plasma, and combined plasma–catalyst treatment of toluene.

plasma–catalyst treatment at all temperatures studied, however, is always less than the linear combination of the plasma alone and catalyst alone treatments.

Some insight into the interaction between the catalyst and plasma can be seen in the time-course data for a single experiment. In Fig. 8, the first 10 min of data represents toluene removal by the catalyst alone. When plasma is turned on, the toluene concentration increases, with a corresponding decrease in CO_2 concentration. After the plasma is turned off, toluene concentration first increases, and then slowly returns to the level seen for the catalyst alone case after approximately 30 min. This implies that the plasma somehow interrupts the normal operation of the catalyst. This interruption is a function of temperature. At 160 °C, the time for toluene concentration to return to the level seen before the plasma was turned on is less than the time resolution of the experiment, and at 150 °C, that time is less than 5 min. In the plasma–catalyst experiments, the removal of toluene by the plasma is presumably equivalent to that removed in the plasma alone experiments since the plasma is located upstream of the catalyst. If this assumption is true, then the plasma, or products of toluene degradation in plasma, completely interrupts all reactions on the catalyst which lead to toluene removal for catalyst alone experiments in the 130 and 140 °C experiments. At 150 and 160 °C, higher rates of adsorption, desorption and surface reaction are able to compensate somewhat for the inhibiting effect of the compounds produced in the plasma.

Another important aspect of the toluene experiments is the fate of the removed toluene. Figs. 9–11 show the concentrations of CO_2, CO, and an unknown byproduct, respectively; these data correspond to experiments for the toluene data

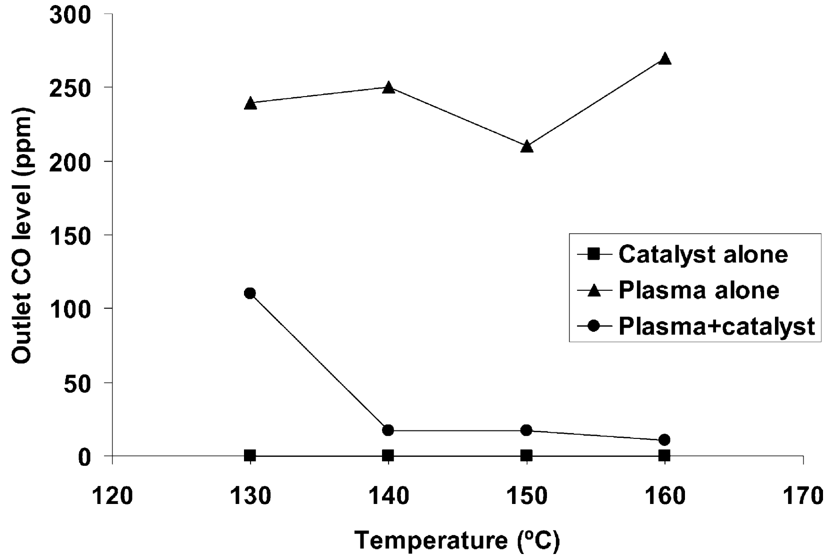

Fig. 10. CO concentration at reactor outlet for catalyst, plasma, and combined plasma–catalyst treatment of toluene.

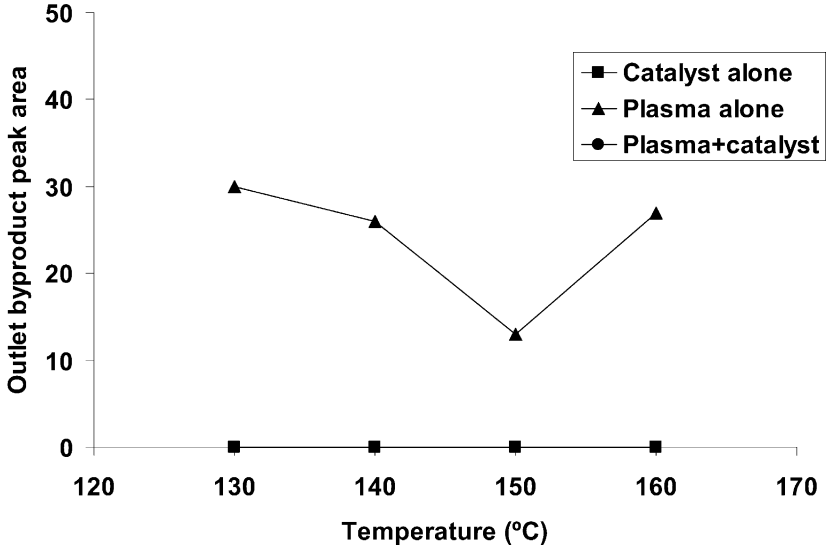

Fig. 11. Unknown byproduct data at reactor outlet for catalyst, plasma, and combined plasma catalyst treatment of toluene. This or some other byproduct of toluene degradation could be responsible for catalyst deactivation.

shown in Fig. 7. The level of CO_2 seen in some of these experiments exceeds that which is expected from the stoichiometry of the removed toluene. There is no evidence that the elevated CO_2 arises from reactions of the RVC with the plasma since control experiments without the addition of organic produce no CO_2 at any temperature. In addition, without plasma CO_2 is not detected at the reactor outlet up to 260 °C with synthetic air (no organic or CO_2) as the feed gas. However, the elevated levels of CO_2 are observed only when organic is present at high temperature with catalyst. Thus, the possibility remains that reactions of toluene and/or toluene byproducts on the catalyst surface lead to oxidation of the carbon substrate, thereby elevating the outlet CO_2 level. Despite the issues regarding the CO_2 levels, the relative amounts of CO_2 and CO observed in the different experiments are notable. Under plasma only operation, CO levels exceed those of CO_2 significantly, and the selectivity toward CO_2 for the catalyst and plasma–catalyst cases greatly exceed that of the plasma alone case, as seen in Fig. 12.

Another aspect of the plasma alone experiments is the fact that some portion of the removed carbon ends up in the form of a solid brown-colored deposit in the reactor. The amount of this material produced and the carbon content have not been measured, and so an adequate carbon balance for the plasma alone experiments is not possible at this time. Presumably, this material is oxidized in the combined plasma–catalyst experiments because a higher percentage of the carbon from the removed toluene is detected as carbon dioxide in these experiments. The formation of a solid byproduct was also observed by Demidiouk et al. [38], who

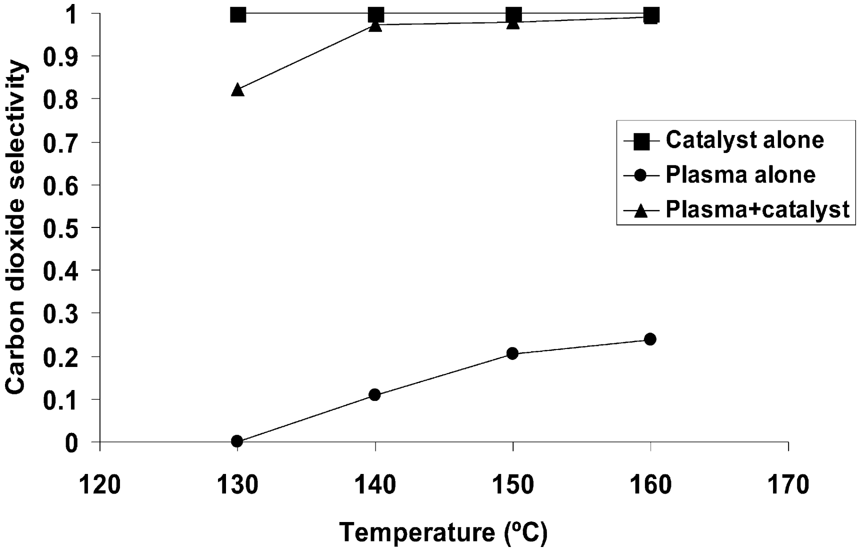

Fig. 12. Selectivity toward CO_2 defined as $CO_2/(CO + CO_2)$ for catalyst, plasma, and combined plasma–catalyst treatment of toluene.

saw at most 20% of the removed toluene converted to CO_2. Another study by Li et al. [39] showed some synergy of corona treatment of toluene with TiO_2 photocatalyst, but made no mention of solid byproduct or inhibition of catalyst activity. Parissi et al. report in [2] some details of the solid material formed and of the size range of aerosols they measured in the treatment of toluene by DBD plasma. Infrared analysis shows the presence of carbonyl and carboxylic acid groups in the deposit and they report that aerosols observed are similar to those observed in conventional combustion processes.

4. Conclusions

Experiments using plasma, platinum–rhodium coated RVC catalyst electrodes, and combined plasma–catalyst treatments of three different gas mixtures showed widely different behavior depending upon the species under consideration. In the absence of plasma, this catalyst is active at higher temperatures in the degradation of toluene and acetonitrile. In the presence of plasma and catalyst, toluene appears to form byproducts that reduce the activity of the catalyst while the removal of acetonitrile by catalyst is unaffected by the plasma. Acetonitrile is partially removed by the plasma, however, the removal in the combined plasma catalyst case is a linear combination of the removal in the two individual cases. The effect of the plasma catalyst combination on NO removal suggests that a more complicated interaction is at work wherein the plasma oxidizes NO to NO_2 and the downstream catalyst then reduced some of the NO_2 back to NO. Future work on this topic will consist of concentration variation for rate law determination, the reversal of flow in the reactor, and separation of the catalyst from the plasma region.

Acknowledgements

We gratefully acknowledge the financial support from the Department of Chemical Engineering, FAMU-FSU College of Engineering, Florida State University and the National Science Foundation, grant No. INT 0086351. Discussions and laboratory assistance from Mayank Sahni, Austin Appleton, and Professor Ronald Clark were also very helpful in the conduction of this work.

References

[1] R.M. Heck, R.J. Farrauto, Catalytic Air Pollution Control: Commercial Technology, Van Nostrand, Reinhold, 1995.
[2] E.M. van Veldhuizen, Electrical Discharges for Environmental Purposes, Fundamentals and Applications, Nova Science Publishers Inc., Huntington, New York, 2000.
[3] S. Masuda, H. Nakao, IEEE Trans. Ind. Appl. 26 (1990) 374.
[4] A. Mizuno, J.S. Clements, USA Patent 4,695,358 (issued on September 22, 1987), to Florida State University.
[5] M.B. Chang, M.J. Kushner, M.J. Rood, Environ. Sci. Technol. 26 (1992) 777.
[6] S.K. Dhali, I. Sardja, J. Appl. Phys. 69 (1991) 6319.
[7] T. Hammer, Poster Presentation at the 1998 Pan American Workshop on Commercialization of AOTs, London, Ontario, 1998.
[8] T. Fujiwara, K. Takaki, Proceedings of the Asia-Pacific Workshop on Water and Air Treatment by Advanced Oxidation Technologies: Innovation and Commercial Applications, AIST Tsukuba Research Center, December 17–19, 1998.
[9] O. Tokunaga, N. Suzuki, Rad. Phys. Chem. 24 (1984) 145.
[10] O. Tokunaga, H. Namba, K. Hirota, in: B.M. Penetrante, S.E. Schultheis (Eds.), Non-thermal Plasma Techniques for Pollution Control, Springer-Verlag, Berlin, 1993, p. 55.
[11] N.W. Frank, Rad. Phys. Chem. 45 (1995) 989.
[12] T. Oda, T. Kato, T. Takahashi, K. Shimizu, IEEE Trans. Ind. Appl. 34 (1998) 268.
[13] K. Shimizu, T. Oda, IEEE Trans. Ind. Appl. 35 (1999) 1311.
[14] J. Hoard, M.L. Balmer, R. Tonkyn, A. Kim, S. Yoon, D. Jimenez, T. Orlando, S.E. Barlow, SAE Technical Paper Series No. 982511, 1998.
[15] M.J. Kirkpatrick, W.C. Finney, B.R. Locke, SAE Technical Paper Series No. 2000-01-2968.
[16] T. Hammer, T. Kishimoto, H. Miessner, R. Rudolph, SAE Technical Paper Series No. 1999-01-3632.
[17] J. Hoard, M.L. Balmer, SAE Technical Paper Series No. 982429, 1998.
[18] T. Yamamoto, K. Mizuno, I. Tamori, A. Ogata, M. Nifuku, G. Michalska, Prieto, IEEE Trans. Ind. Appl. 32 (1996) 100.
[19] Y.H. Song, K.T. Kim, H.J. Yi, S.J. Kim, SAE Technical Paper Series No. F2000H224.
[20] H. Miessner, K.P. Francke, R. Rudolph, Appl. Catal. B 36 (2002) 53.
[21] K.P. Francke, H. Miessner, R. Rudolf, Plasma Chem. Plasma Process. 20 (2000) 393.
[22] U. Roland, F. Holzer, F.D. Kopinke, Catal. Today 73 (2002) 315.
[23] D. Li, D. Yakushiji, S. Kanazawa, T. Ohuubo, Y. Nomoto, J. Electrostat. 55 (2002) 311.
[24] Y.H. Song, S.Y. Han, M.S. Cha, K.T. Kim, K. Choi, S.J. Kim, Proceedings of the Third International Symposium on Non-thermal Plasma Technology for Pollution Control, Cheju Island, Republic of Korea, 2001, p. 274.
[25] A. Ogata, K. Yamanouchi, K. Mizuno, S. Kushiyama, T. Yamamoto, Plasma Chem. Plasma Process. 19 (1999) 383.
[26] K.P. Francke, H. Miessner, R. Rudolph, Catal. Today 59 (2000) 411.
[27] H.H. Kim, K. Tsunoda, S. Katsura, A. Mizuno, Proceedings of the IEEE Industry Application Society Annual Meeting, New Orleans, LA, October 5–9, 1997.
[28] H.H. Kim, K. Tsunoda, K. Shimizu, S. Tanaka, T. Yamamoto, A.J. Mizuno, Adv. Oxid. Technol. 4 (1999) 1.
[29] F. Holzer, U. Roland, F.D. Kopinkie, Appl. Catal. B 38 (2002) 163.
[30] J. Wang, Electrochem. Acta 26 (1981) 1721.
[31] M. Kirkpatrick, W.C. Finney, B.R. Locke, IEEE Trans. Ind. Appl. 36 (2000) 500.
[32] L.N. Krasnoperov, L.G. Krishtopa, Proceedings of the Third International Symposium on Non-thermal Plasma, Cheju Island, Republic of Korea, 2001.
[33] R.G. Tonkyn, S.E. Barlow, J.W. Hoard, Appl. Catal. B 40 (2003) 207.
[34] C. Liu, J. Wang, K. Yu, B. Eliasson, O. Xia, B. Xue, Y. Zhang, J. Electrostat. 54 (2002) 149.
[35] H. Meissner, K.P. Francke, R. Rudolph, T. Hammer, Catal. Today 2732 (2002) 1.
[36] G. Sathiamoorthy, S. Kalyana, W.C. Finney, R.J. Clark, B.R. Locke, Ind. Eng. Chem. Res. 38 (1999) 1844.
[37] J. Kaspar, P. Fornasiero, N. Hickey, Catal. Today 77 (2003) 419.
[38] V. Demidiouk, S.I. Moon, J.O. Chae, Catal. Commun. 4 (2003) 51.
[39] D. Li, D. Yakushiji, S. Kanazawa, T. Ohkubo, Y. Nomoto, J. Electrostat. 55 (2002) 311.